ELSEVIER

Journal of Hazardous Materials 60 (1998) 175–203

JOURNAL OF HAZARDOUS MATERIALS

Chemical compatibility study of geomembranes—sorption/desorption, diffusion and swelling phenomena

T.M. Aminabhavi *, H.G. Naik

Department of Chemistry, Karnatak University, Dharwad 580 003, India

Received 17 July 1997; revised 30 December 1997; accepted 9 January 1998

Abstract

Sorption/desorption results of *n*-alkanes into high density polyethylene, linear low density polyethylene, very low density polyethylene and polypropylene geomembranes are presented at 25, 50 and 70°C. Sorption results are obtained by a gravimetric method and diffusion coefficients have been calculated by using Fick's equation from the initial linear portions of the sorption/desorption curves. Swelling of the geomembranes was studied from a measurement of the increase in volume, thickness and diameter. From a temperature dependence of sorption and diffusion coefficients, the Arrhenius parameters have been calculated. Liquid concentration profiles have been computed using Fick's equation for the appropriate initial and boundary conditions. The results of this study may have relevance in selecting the suitable geomembrane for a specific application in hazardous waste chemical ponds and other similar situations.

Keywords: Geomembrane; Sorption; Diffusion; Swelling

1. Introduction

Polymeric geomembranes are the nonporous materials which are impermeable to organic liquids and other leachates [1–8]. These are used as liners for the containment of hazardous or municipal wastes in conjunction with geotextiles or mesh underliners which reinforce or protect the more flexible geomembrane whilst at the same time acting as an escape route for gases and leachates generated in certain wastes. The range of

* Corresponding author. Fax: +91-836-747884; e-mail: karuni@bom2.vsnl.net.in

0304-3894/98/$19.00
PII S0304-3894(98)00090-9

geomembrane products and their applications has expanded rapidly over the past decade [9]. Selecting a liner involves defining the site requirements, length of storage and hazardous waste to be contained. Failure in geomembrane performance will occur due to chemical attack and hence, its resistance to hazardous chemicals from a study of sorption/desorption and diffusion properties are important in selecting a geomembrane [10]. Because of differences in chemical structure, crosslinking, etc. geomembranes vary widely in their resistivity to a given chemical and therefore their chemical resistivity testing is to be performed.

The geomembranes find applications as solid and liquid containments such as hazardous waste landfills and caps, ponds, lagoons and reservoirs, mining heap, beach pads, failings, impoundments, solution channels, industrial sites, floating covers, etc. Of these, the high density polyethylene (HDPE), linear low density polyethylene (LLDPE), very low density polyethylene (VLDPE) and polypropylene (PP) are important. However, these, HDPE is one of the most widely used geomembranes for tank linings and sludge pond as it provides good chemical resistance and impermeability in addition to its exceptional ultraviolet light resistance and excellent mechanical strength. The LLDPE and VLDPE geomembranes have also been used frequently [9,10]. Approximately 80% of all geosynthetics are made from polypropylene. The wide uses of geomembranes as effective barriers between the organic pollutants under varied environmental conditions and the fertile soil require a precise determination of sorption/desorption and diffusion properties by the test methods that are appropriate to service conditions. Geomembranes, are known to permeate liquids on a molecular level by the process of sorption and diffusion [4–6,9,10]. Desorption is also an important inherent property of the geomembrane materials.

The principal objective of this study is to present some useful experimental data on the resistivity of HDPE, LLDPE, VLDPE and PP geomembranes to *n*-alkanes that are frequently found in landfill and impoundment sites. Sorption results at 25, 50 and 70°C and the desorption data at 25°C have been obtained by the gravimetric sorption technique. From the sorption and desorption data, diffusion coefficients have been calculated using Fick's equation [11]. The temperature dependence of sorption and diffusion coefficients has been studied using Arrhenius equation to estimate the activation parameters. Furthermore, the concentration profiles of liquids into geomembranes have been calculated. Such a database would be a useful source index to the liner manufacturers, vendors, purchasers and reviewers of permit applications to select the most chemically resistant geomembrane for a given waste site application.

2. Experimental

2.1. Chemicals

The *n*-alkanes used in this research are: hexane, heptane, nonane, dodecane and pentadacane (all were of analytical reagent grade samples supplied from S.D. Fine Chemicals, Mumbai, India).

Table 1
Some typical properties of geomembranes used

Property	Method	Units	Geomembranes			
			PP	VLDPE	LLDPE	HDPE
Thickness	ASTM D 751, NSF model	mm	1.085	1.06	1.08	1.59
Density	ASTM D 1505	g/cm^3	0.91	0.922	0.928	0.948
Carbon black content	ASTM D 1603	%	2.3	2.5	2.3	2.35
Tensile properties	ASTM D 638					
Stress at yield		MPa	–	11.6	–	17.6
Stress at break		MPa	18.8	32.6	35.2	33.4
Strain at yield	1.3 in. gauge length (NSF)	%	–	20.5	–	16.9
Strain at break	2.0 in. gauge or extensometer	%	–	1000	–	890
Modulus of elasticity	ASTM D 638	MPa	–	571	–	931
100% Secant modulus		MPa	10.8	–	–	–
Dimensional stability	ASTM D 1204, NSF model	%	0.4	1.1	0.6	0.4
Tear resistance	ASTM D 1004	N/cm	692	1505	1243	1050
Puncture resistance	ASTM D 4833	N/cm	2058	3542	4098	3728
Water absorption	ASTM D 570 at 23°C	%	–	0.04	–	0.05
Water vapor transmission	ASTM E 96	g/day m^2	–	0.174	–	0.009

2.2. Geomembranes

The PP, LLDPE, VLDPE and HDPE geomembranes used were fabricated at NSC Research Center, Galesburg, IL, USA in sheets with dimensions of 28 cm × 22 cm × 0.110 cm, 35 cm × 30 cm × 0.106 cm, 35 cm × 30 cm × 0.109 cm and 35 cm × 30 cm × 0.160 cm, respectively. Some typical properties of these geomembranes are summarized in Table 1.

2.3. Sorption / desorption measurements

In our experimental approach, the geomembrane is exposed to the challenge chemical for a definite period of time and the changes in mass of the samples as well as dimensions are measured. These samples absorb liquids depending upon the polymer network structure. From these experiments, mass gain due to sorption or mass loss due to desorption as well as swelling of the geomembranes are accurately monitored as a function of time. These data are then used to calculate diffusion and sorption coefficients of the migrating chemicals inside the geomembrane [12–18] [19–24].

Sorption experiments were performed at 25, 50 and 70°C using an electronically controlled oven (WTB Binder, Germany) maintained at the desired temperature within the accuracy of ±0.5°C. The circularly cut disc-shaped samples of geomembrane having the diameter of ≈2.00 cm were kept in vacuum oven at 25°C for 48 h before experimentation. These samples were exposed to *n*-alkanes (20–30 cm^3) by placing them inside the screw-tight test bottles which were maintained at the desired temperature within the accuracy of ±0.5°C. The test bottles were placed inside the oven that was calibrated previously with a quartz thermometer for precise temperature control. The

Table 2
Sorption coefficients (S in wt.%) for geomembranes with *n*-alkanes

n-Alkanes	Temperature (°C)	PP	VLDPE	LLDPE	HDPE
Hexane	25	181.63	17.42	15.36	6.59
	50	240.84 (69.13)	31.60 (14.31)	22.18 (11.36)	9.87 (7.30)
Heptane	25	185.86	16.03	13.52	6.82
	50	252.65	32.82	22.27	9.87
	70	320.75 (74.59)	68.91 (14.08)	36.72 (11.04)	13.61 (5.37)
Nonane	25	178.75	16.10	12.62	6.42
	50	252.51	32.42	21.62	9.45
	70	315.51 (87.01)	76.31 (13.92)	36.56 (10.64)	12.92 (5.01)
Dodecane	25	159.35	15.67	12.39	6.12
	50	229.02	28.90	19.38	8.91
	70	296.84 (27.58)	62.26 (13.61)	32.93 (8.582)	11.84 (4.39)
Pentadecane	25	135.56	19.55	15.19	6.32
	50	229.70	32.85	17.41	10.33
	70	267.83 (13.90)	49.38 (12.99)	28.62 (7.17)	10.85 (1.95)

Values in the parentheses are desorption coefficients at 25°C.

weight measurements were done at suitably selected time intervals by removing the samples and wiping the surface adhered solvent drops in-between filter paper wraps. The samples were then placed on a top-loading single pan digital Metler balance (Model AE 240, Switzerland) sensitive to ± 0.01 mg and the mass measurements were taken.

The total time spent by the geomembrane outside the solvent container was kept within 20–30 s in order to minimize the possible experimental error. This error was found to be negligible considering the small amount of time spent (30 s or even less) by the membrane outside the test bottle. The desorption runs were performed by keeping the already sorbed samples in a vacuum controlled oven at 25°C under the atmospheric pressure. The mass loss of the samples was monitored at regular intervals of time by removing them from the oven and weighing in the same manner as was done in sorption experiments. When the samples attained equilibrium sorption or desorption, no more mass gain or loss occurred and this did not change significantly by keeping the samples inside the containers for a further period of one or two days.

The weight percent increase C_t, as a function of time, t is calculated as:

$$C_t = \left(\frac{W_t - W_0}{W_0} \right) \times 100 \quad (1)$$

where W_0 is initial weight of the sample and W_t is its weight at time t, for the immersion period. These data are given in Table 2. The weight percent decrease for desorption was calculated similarly using Eq. (1).

3. Estimation of solvent diffusion coefficients from sorption data

Chemical resistivity of a geomembrane is related to its ability to perform the intended function during or after contact with a liquid. If no change occurs in liner's ability to

function as designed after chemical exposure, it is said to be resistant to the chemical. Even though geomembranes are nonporous, liquids, gases and vapors of liquids can permeate through it on a molecular level. Thus, even if a geomembrane is free of voids, some liquids may permeate through it in order to escape out of the containment unit. In a way the geomembranes are permeable to organic liquids to some extent and therefore an assessment of the diffusivity of liquids through these materials is important. However, the basic transport mechanism in these processes is essentially the same for all the permeating molecules [11–18] [19–25].

Several methods have been developed in the literature to estimate the ability of a geomembrane to act as an effective barrier to an aggressive chemical [4–8]. In most of these studies, Fickian diffusion theory is used which emphasizes the prediction of diffusion coefficient of a liquid in a polymer. Critical review of the applicability and reliability of such test methods have been given elsewhere [9]. However, a study of the concentration dependence of D for polymer–solvent systems has also been made [24]. Theoretical approaches to estimate diffusion coefficients involve the application of free volume theory [26,27]. Although these models provide a good qualitative representation of the variations of D with temperature and liquid concentration, it is difficult to apply them because they require physical property data that are not generally available. Consequently, these approaches are not suitable in the present study. Therefore, we have used Fick's diffusion equation to estimate the diffusion coefficient [11]:

$$\frac{\partial C}{\partial t} = D\left(\frac{\partial^2 C}{\partial x^2}\right) \tag{2}$$

where $C = C(x, t)$ is liquid uptake in weight percent, D is diffusion coefficient in cm^2/s and x is sample thickness in cm. Eq. (2) can be solved for concentration-independent diffusivity, D as [11]:

$$D = \pi\left(\frac{h\theta}{4C_\infty}\right)^2 \tag{3}$$

where C_∞ is equilibrium weight uptake at $t \to \infty$, θ is slope of the initial linear portion of the sorption/desorption curves; h is membrane thickness. The sorption/desorption data initially vary linearly with time up to about 50–55% attainment of equilibrium saturation.

For a successful application of geomembranes it is essential to know the liquid concentration profiles of the migrating chemicals. This was done by solving the one dimensional Fick's diffusion equation using the following assumptions [25]:

1. liquid diffusion into the geomembrane takes place in the x-direction only,
2. sorption takes place under transient conditions with a constant diffusivity,
3. during sorption, when the geomembrane is exposed to solvent, its concentration on the membrane surface reaches equilibrium immediately,
4. time required for the geomembrane to establish thermal equilibrium is negligible when compared to the time of sorption, and
5. changes in geomembrane dimensions are negligible during its liquid exposure time.

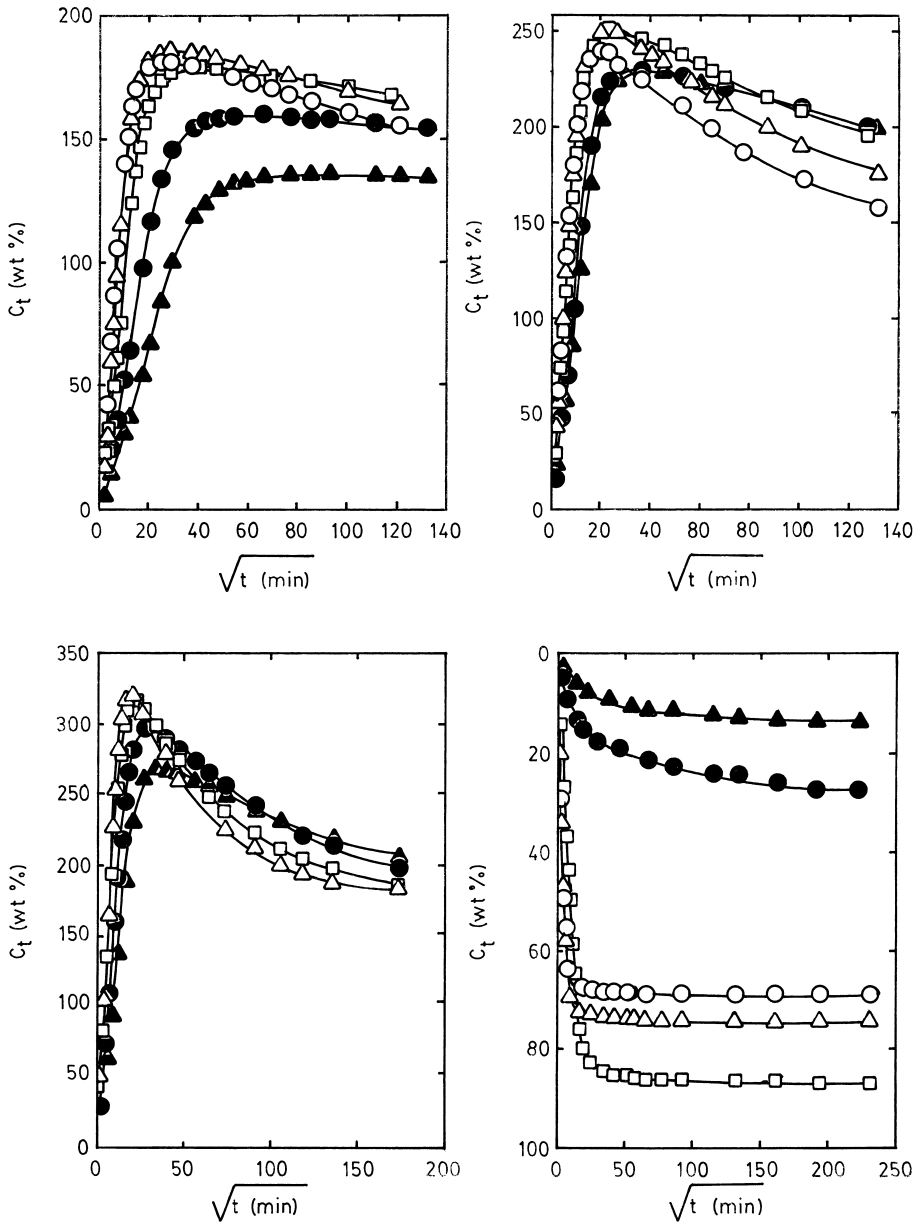

Fig. 1. Sorption curves i.e. wt.% uptake (C_t) vs. square root of time ($t^{1/2}$) for PP geomembrane with (○) hexane, (△) heptane, (□) nonane, (●) dodecane, (▲) pentadecane at (A) 25°C, (B) 50°C, (C) 70°C, and (D) desorption curves at 25°C.

Eq. (3) can be solved for the following initial and boundary conditions,

$$t = 0 \quad 0 \le x \le h \quad C = 0 \tag{4}$$

$$t \ge 0 \quad x = 0, \quad x = h \quad C = C_\infty \tag{5}$$

$$\frac{\partial C}{\partial x} = 0 \quad x = 0, \quad t > 0 \tag{6}$$

to yield an equation for solvent uptake ($C_{x,t}$) inside the geomembrane of thickness h, at time t and distance, x as [25]:

$$\frac{C_{(x,t)}}{C_\infty} = 1 - \frac{4}{\pi} \sum_{m=0}^{\infty} \frac{1}{(2m+1)} \exp\left[- \frac{D(2m+1)^2 \pi^2 t}{h^2} \right] \sin\left[\frac{(2m+1)\pi x}{h} \right] \tag{7}$$

where m is an integer. Solving Eq. (7), we get concentration profiles of the migrating liquids developed within the geomembrane. These data are useful to study the liquid migration as a function of time and penetration depth of the liquid from face to the middle of the geomembranes along the thickness direction.

4. Results and discussion

4.1. Sorption / desorption kinetics

Sorption results of *n*-alkanes with PP geomembrane expressed in weight percent units at 25, 50 and 70°C as well as desorption data at 25°C are presented in Fig. 1. It is observed that at 25°C, sorption curves for lower alkanes viz., hexane, heptane and nonane are higher than those observed for dodecane and pentadecane. Also, for lower alkanes the curves reach maxima much faster than the higher alkanes. However, after attainment of equilibrium sorption, a slow decrease in sorption is observed at 25°C for lower alkanes only. At 50 and 70°C all the alkanes show a decrease in sorption values after attainment of equilibrium. This type of decrease in sorption is due to the fast desorption of liquids from the PP geomembrane. The desorption curves of lower alkanes show a rapid decline than higher alkanes. The sorption and desorption results do not show any systematic variation with the size of *n*-alkanes. In general, equilibrium sorption values show an increase with increase in temperature for all the alkanes. Dodecane and pentadecane require longer time for sorption as well as desorption than the lower alkanes. In all the cases and at all the temperatures, sorption curves follow a Fickian transport i.e. no sigmoidal trends are observed. At 70°C, the sorption curves exhibit an overshoot effect suggesting an immediate burst effect of alkane molecules within the pores of geomembrane matrices. Sorption results for hexane at 70°C are not presented due to its lower boiling temperature.

In Fig. 2 are presented the sorption/desorption results of VLDPE geomembrane vs. alkanes. At 25 and 50°C, the sorption tendencies of pentadecane follow a two-step function possibly because of the difficulty involved in its transport as a result of its larger size than the other alkanes. However, at 70°C a decrease in sorption values is

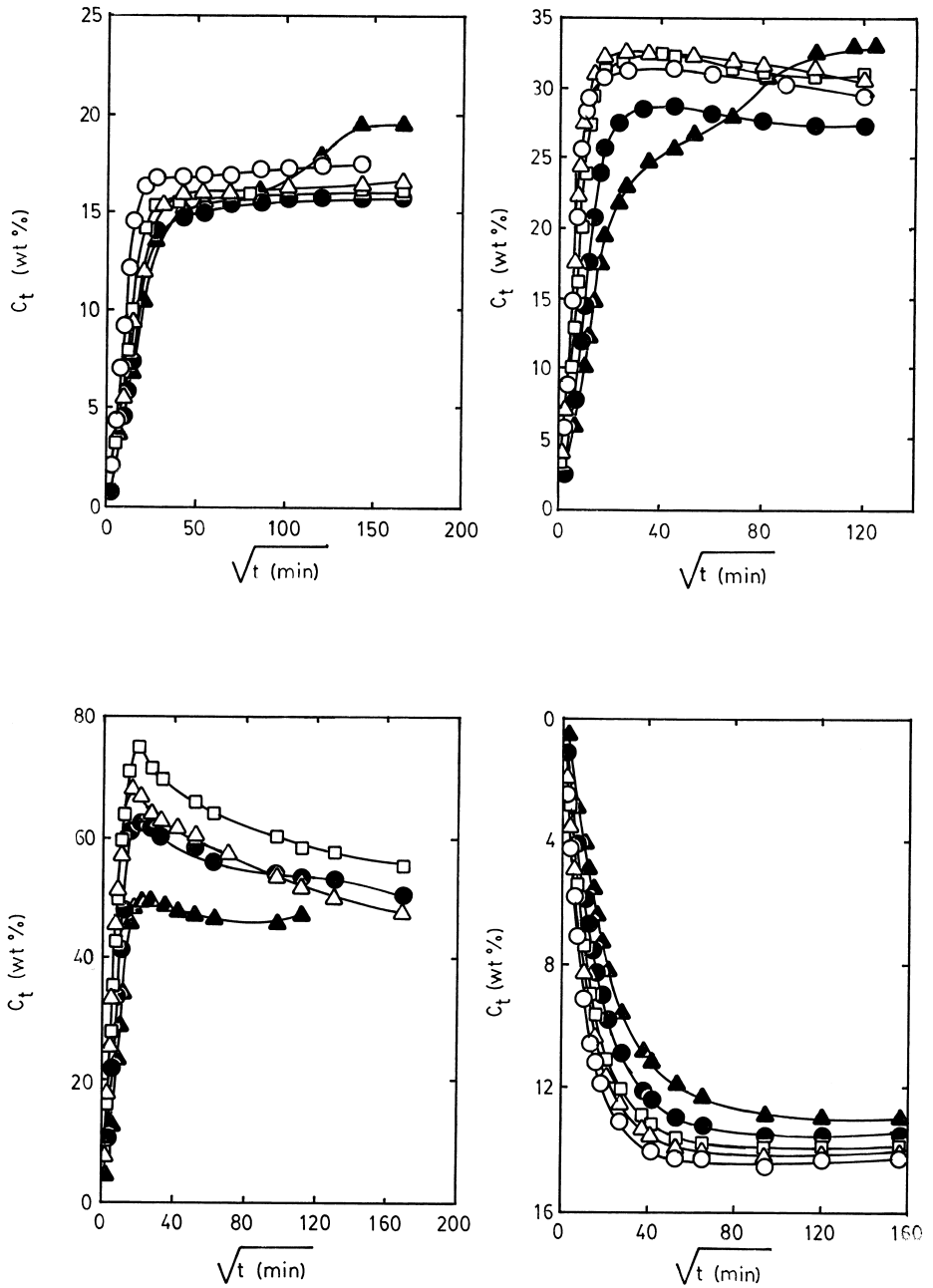

Fig. 2. Sorption curves i.e. wt.% uptake (C_t) vs. square root of time ($t^{1/2}$) for VLDPE geomembrane at (A) 25°C, (B) 50°C, (C) 70°C, and (D) desorption curves at 25°C for the same solvents as given in Fig. 1.

observed for all the alkanes. In all the cases, sorption does not follow any systematic trend with the size of alkanes. On the other hand, desorption curves for VLDPE geomembrane vary systematically with the size of *n*-alkanes i.e. lower alkanes desorb much faster than the higher alkanes. The absence of sigmoidal trends for the VLDPE geomembrane suggests the presence of Fickian transport. The sorption/desorption results for LLDPE geomembrane + *n*-alkanes are presented in Fig. 3. It is found that the sorption curves at 25°C follow a systematic trend with the size of alkanes i.e. sorption results for hexane are higher and these values decrease with increasing size of alkanes. The sorption curve for pentadecane is increasing monotonically with time. However, at 50°C sorption curves for lower alkanes vary almost identically, whereas for dodecane and pentadecane the sorption curves show a Fickian trend. At 70°C, the sorption curves of heptane and nonane are quite identical, but for higher alkanes, these are different. Another characteristic property of the curves at 70°C is that a slow decrease in sorption is observed indicating a quick desorption of the liquids from the geomembrane. The desorption curves in Fig. 3 show a systematic trend with the size of alkanes i.e. lower alkanes desorb faster than the higher alkanes.

In Fig. 4 are presented the sorption/desorption curves for *n*-alkanes with HDPE, which is considered to be one of the toughest and most widely used geomembranes in chemical pond lining applications. It also is known to exhibit least sorptivity for many liquids, a reputation upheld in this study. For HDPE, sorption curves at 25 and 70°C show more sigmoidal trends than at 50°C; the curve for pentadecane exhibits a double-step increase at 50°C. The observed sigmoidal shapes are further indicative of the slow migration of *n*-alkanes in HDPE geomembrane. The variations in sorption curves follow a systematic dependence on the size of *n*-alkane molecules only at 70°C. However, at 25 and 50°C no systematic variation of sorption curves is observed with the size of alkanes. For instance, at 25°C the curves for hexane and nonane show a steady decline after reaching equilibrium. Similarly, at 50°C the sorption curves for hexane and heptane are almost identical. Therefore, a single curve is drawn to show the dependence for both hexane and heptane. The desorption curves presented in Fig. 4 exhibit a systematic dependence on the size of *n*-alkanes. Compared to all *n*-alkanes, pentadecane shows a least desorptivity.

Fig. 5 displays a comparison between different geomembranes for the transport of hexane and pentadecane at 25°C. Wide variations in the sorption of PP geomembrane are observed when compared to other geomembranes. Similar types of dependencies are shown in Figs. 6 and 7 at 50 and 70°C, respectively.

In order to confirm whether the samples have attained complete equilibration or not, the geomembranes were kept immersed in the respective liquids over an extended period of one or two days beyond the equilibrium saturation times. From the equilibrium values sorption coefficients, S were calculated in weight percent units. These data are presented in Table 2. The sorption results show a systematic variation depending upon the type of geomembrane and the alkanes used. For instance, HDPE geomembrane shows least sorptivity, whereas for LLDPE and VLDPE geomembranes sorption is higher than HDPE. In the case of PP geomembrane, sorption is higher than all the other polyethylene-based geomembranes (HDPE, LLDPE and VLDPE). Sorption results decrease with increasing molecular size of *n*-alkanes i.e. from hexane to pentadecane for the

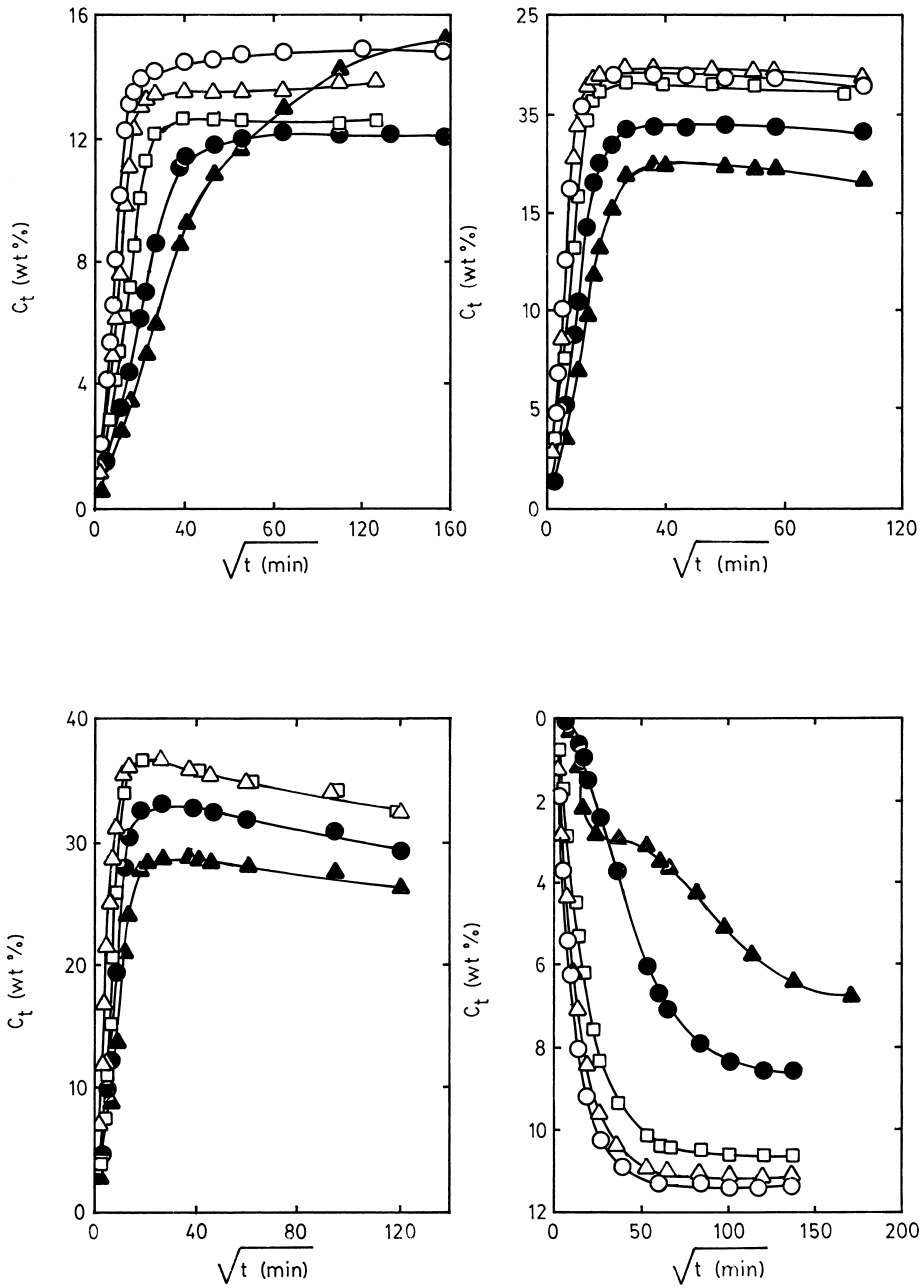

Fig. 3. Sorption curves i.e. wt.% uptake (C_t) vs. square root of time ($t^{1/2}$) for LLDPE geomembrane at (A) 25°C, (B) 50°C, (C) 70°C, and (D) desorption curves at 25°C for the same solvents as given in Fig. 1.

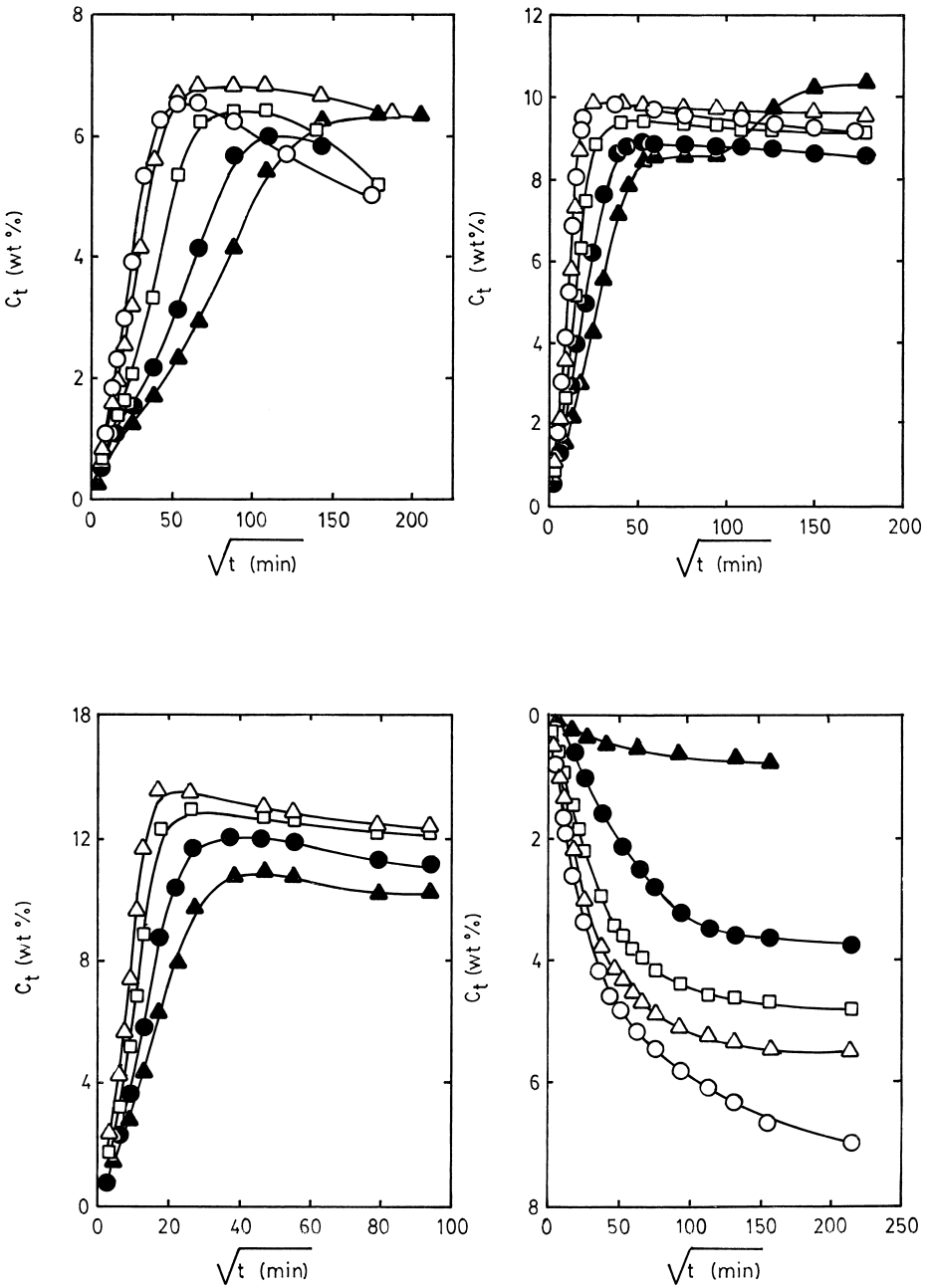

Fig. 4. Sorption curves i.e. wt.% uptake (C_t) vs. square root of time ($t^{1/2}$) for HDPE geomembrane at (A) 25°C, (B) 50°C, (C) 70°C, and (D) desorption curves at 25°C for the same solvents as given in Fig. 1.

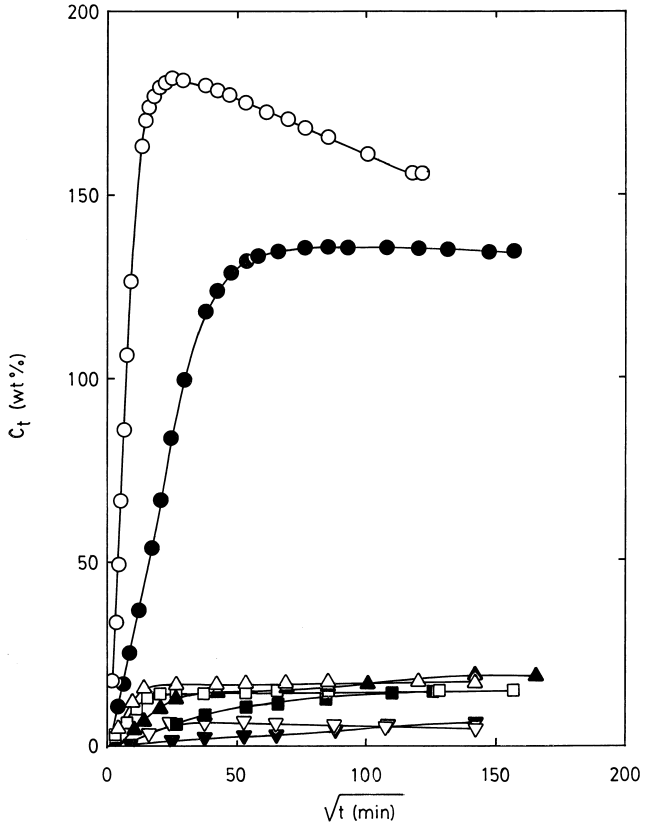

Fig. 5. Sorption curves i.e. wt.% uptake (C_t) vs. square root of time ($t^{1/2}$) for PP (○,●), VLDPE (△,▲), LLDPE (□,■) and HDPE (▽,▼) geomembranes with hexane and pentadecane respectively at 25°C.

geomembranes in the investigated temperature range of 25 to 70°C. With an increase in temperature, sorption also increases and this effect is more significant with PP, VLDPE and LLDPE than with the HDPE geomembrane. From the sorption results presented in Table 2, it may be inferred that HDPE is the most resistant geomembrane and may be recommended as a liner in the environment of *n*-alkanes and that PP geomembrane is not as suitable when compared to polyethylene-based geomembranes. The desorption values at 25°C are also included in Table 2. These values vary in the sequence: PP > VLDPE > LLDPE > HDPE for all the liquids.

The initial sorption results before completion of 50–55% of equilibrium have been analyzed using the empirical relationship [28,29].

$$\frac{C_t}{C_\infty} = Kt^n \tag{8}$$

where, C_t and C_∞ are the same as defined before. The parameter, K represents the

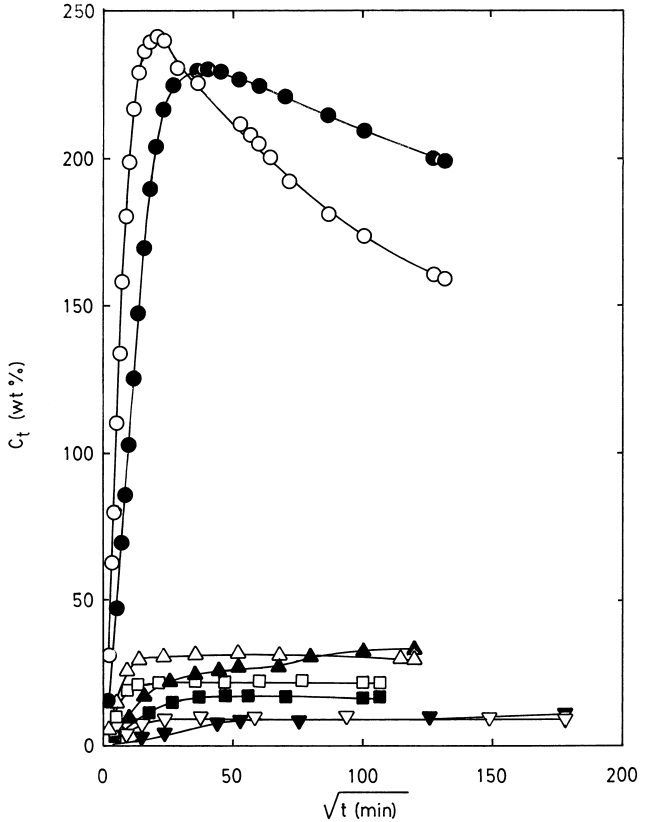

Fig. 6. Sorption curves i.e. wt.% uptake (C_t) vs. square root of time ($t^{1/2}$) for PP (○,●), VLDPE (△,▲), LLDPE (□,■) and HDPE (▽,▼) geomembranes with hexane and pentadecane respectively at 50°C.

extent of interaction between *n*-alkanes and geomembranes, while the exponent value of *n* indicates the type of transport mechanism. The values of *K* and *n* have been calculated using the least-squares procedures, but only the results of *K* are presented in Table 3. It may be noted that the values of *K* also exhibit the trends similar to sorption results i.e. these results vary according to the sequence: HDPE < LLDPE < VLDPE < PP. Thus, sorption results are indicative of the membrane–solvent interactions as manifested in the *K* values. The values of *K* show a systematic increase with increasing temperature. The values of *n* (not included in Table 3) for the present *n*-alkane–geomembrane systems show variations from 0.50 to 0.60 suggesting that transport is of Fickian type. Sorption results presented in Figs. 1–7 also indicate a near linearity in the early stages i.e. up to 50–55% equilibrium sorption, for the mass uptake vs. square root time plots. This further supports that the overall transport is of Fickian type. In the present study, the values of *n* for HDPE geomembrane range between 0.50–0.57; for LLDPE, *n* varies between 0.50–0.59; for VLDPE, it is 0.50–0.59, whereas for PP, *n* values are in the range 0.50–0.60.

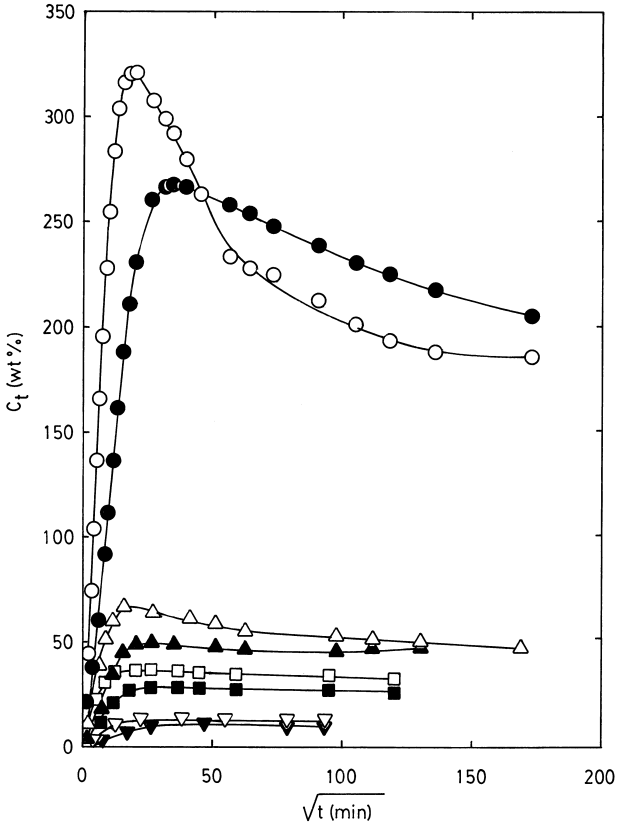

Fig. 7. Sorption curves i.e. wt.% uptake (C_t) vs. square root of time ($t^{1/2}$) for PP (○,●), VLDPE (△,▲), LLDPE (□,■) and HDPE (▽,▼) geomembranes with hexane and pentadecane respectively at 70°C.

4.2. Diffusion

Diffusion coefficients, D calculated from Eq. (3) for *n*-alkanes with the geomembranes are presented in Table 4. In general, the values of D show a systematic dependence on the size of *n*-alkanes as well as the type of the geomembrane. The values of D follow the same pattern as those of S and K discussed before. Diffusion coefficients of all the alkanes in the case of HDPE geomembrane are lower than observed for all the remaining geomembranes. This further confirms that HDPE is most resistant of all. The values of D and K calculated from Eqs. (3) and (8) respectively, from desorption data at 25°C are also included in Tables 4 and 3. It is observed that D and K values for desorption are higher than those observed for sorption in all the cases.

4.3. Concentration profiles

The calculated concentration profiles from Eq. (7) for the high diffusing heptane with all the geomembranes at 25, 50 and 70°C are displayed in Figs. 8–10 respectively. In

Table 3
Results of parameter $K \times 10^2$ (in g/g(min)^n) of Fig. 8 for geomembranes at different temperatures

n-Alkanes	Temperature (°C)	PP	VLDPE	LLDPE	HDPE
Hexane	25	5.5	5.11	4.89	2.18
	50	10.19 (22.12)	8.41 (8.34)	8.16 (8.07)	3.58 (2.99)
Heptane	25	4.79	3.39	3.12	1.64
	50	8.65	7.21	6.79	3.31
	70	13.26 (16.53)	12.36 (6.02)	10.50 (4.56)	4.60 (1.99)
Nonane	25	4.20	3.17	2.85	1.54
	50	6.33	5.49	5.40	2.47
	70	11.56 (10.27)	10.55 (5.07)	5.83 (3.21)	3.30 (0.38)
Dodecane	25	2.68	2.39	2.31	1.33
	50	4.38	4.08	3.70	2.45
	70	8.04 (7.90)	7.60 (3.68)	4.66 (1.04)	2.92 (0.16)
Pentadecane	25	1.82	1.49	1.42	1.26
	50	3.83	3.37	2.72	2.12
	70	6.01 (5.90)	5.42 (1.86)	4.43 (0.23)	3.02 (0.09)

Values in the parentheses are obtained from desorption runs at 25°C.

general, concentration profiles are systematically higher for heptane with increasing temperature and the profiles depend on the type of geomembrane. While calculating the theoretical curves it was not possible to use the same initial times so as to facilitate comparison of the curves under identical conditions and hence, different times were chosen for different membranes. It is gratifying to note that different shapes and different values of the profiles are observed depending upon the nature of the barrier

Table 4
Diffusion coefficients ($D \times 10^7$ cm^2/s) of geomembranes with *n*-alkanes

n-Alkanes	Temperature (°C)	PP	VLDPE	LLDPE	HDPE
Hexane	25	3.91	1.35	1.27	0.70
	50	7.72 (21.4)	4.32 (2.01)	3.33 (1.64)	2.20 (0.29)
Heptane	25	2.30	0.97	0.88	0.43
	50	5.54	3.52	2.56	1.62
	70	8.37 (16.7)	8.09 (1.77)	5.84 (1.41)	3.10 (0.44)
Nonane	25	1.26	0.70	0.53	0.21
	50	2.75	1.93	1.41	1.19
	70	4.71 (3.82)	4.11 (1.08)	3.29 (0.64)	1.99 (0.30)
Dodecane	25	0.49	0.43	0.24	0.07
	50	1.23	1.11	0.99	0.68
	70	2.35 (1.58)	2.21 (0.78)	1.81 (0.07)	0.92 (0.08)
Pentadecane	25	0.32	0.27	0.08	0.04
	50	0.95	0.76	0.53	0.23
	70	1.59 (1.09)	1.43 (0.50)	1.17 (0.02)	0.85 (0.01)

Values in the parentheses are obtained from desorption runs at 25°C.

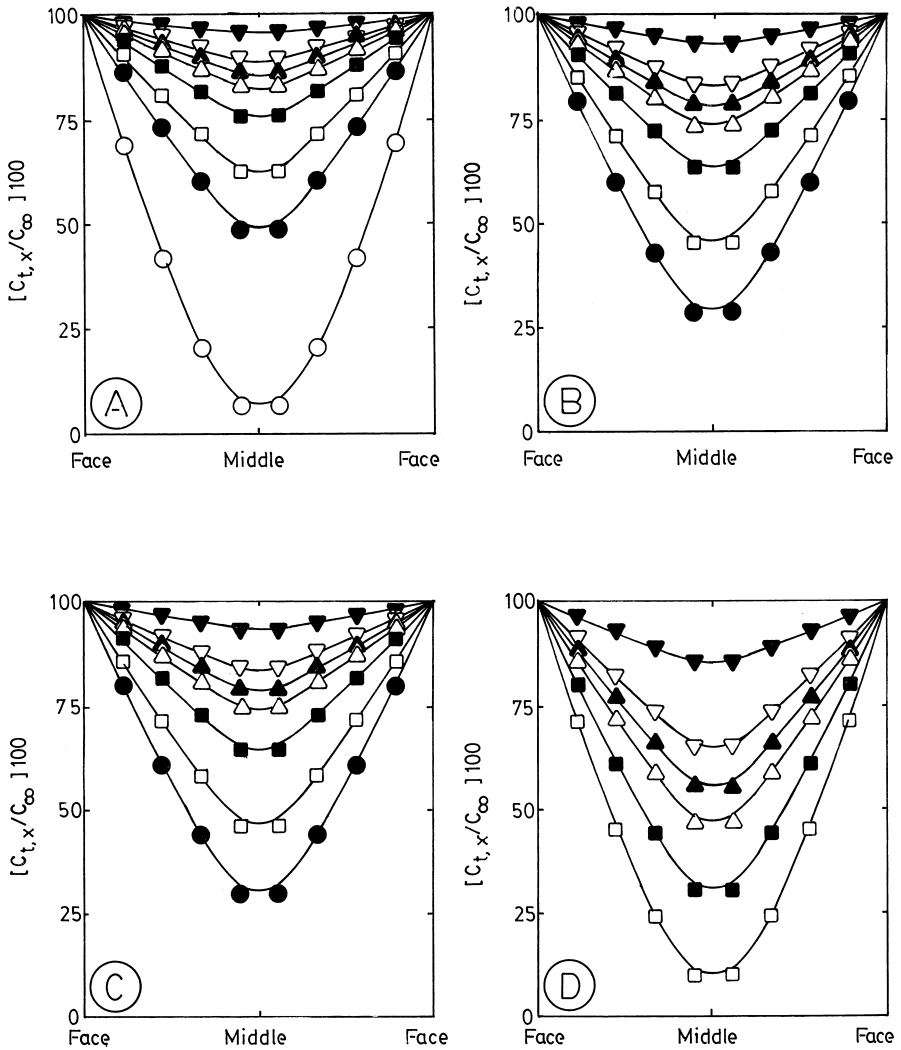

Fig. 8. Concentration profiles calculated from Eq. (7) for heptane at (○) 0.6 min, (●) 4 min, (□) 8 min, (■) 20 min, (△) 40 min, (▲) 60 min, (▽)100 min, (▼) 600 min with (A) PP, (B) VLDPE, (C) LLDPE and (D) HDPE geomembranes at 25°C.

geomembrane. Similar plots are shown for the low diffusing pentadecane in Figs. 11–13 wherein again the same observations are seen as those observed for heptane. In Figs. 14 and 15, a comparison is made between different geomembranes for heptane and pentadecane at 25, 50 and 70°C. For the other alkanes, intermediary values are observed. It is further found that lower values of concentration profiles are observed for PP geomembrane than all the other geomembranes.

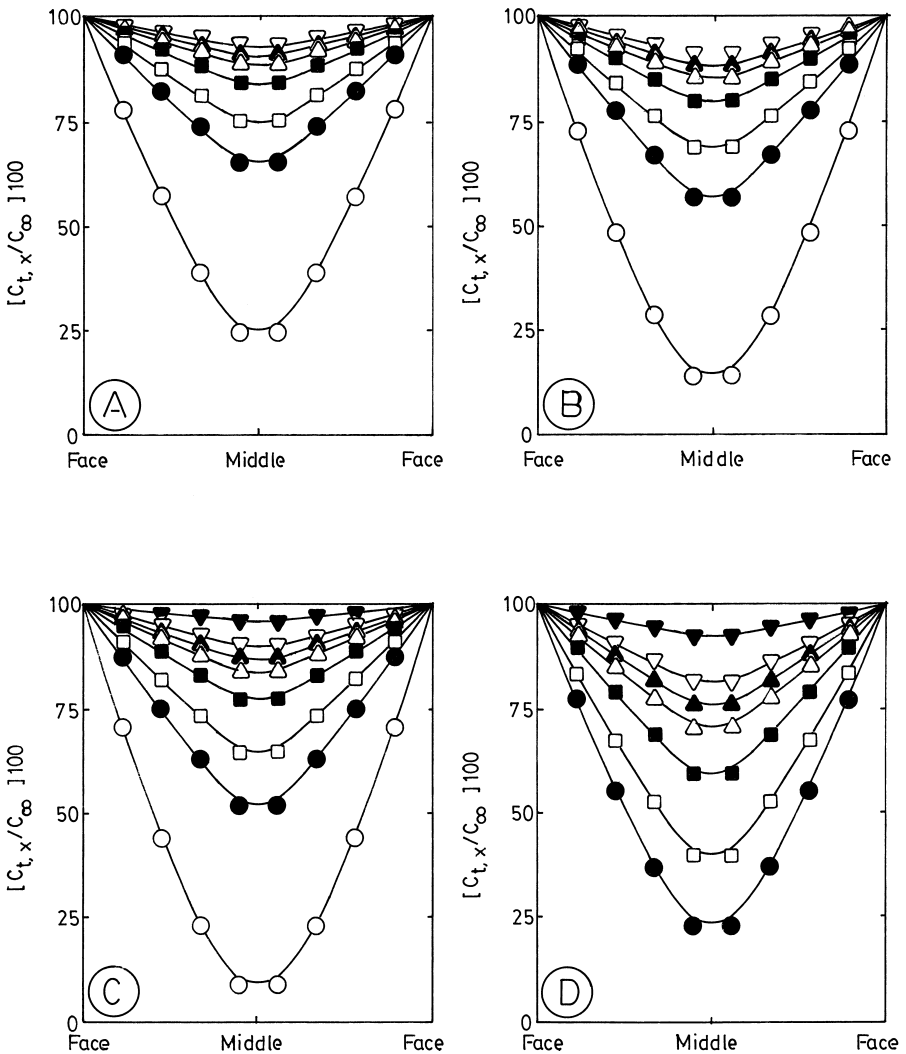

Fig. 9. Concentration profiles calculated from Eq. (7) for heptane with (A) PP, (B) VLDPE, (C) LLDPE and (D) HDPE geomembranes for the same time intervals as in Fig. 8 at 50°C.

4.4. Swelling

Dimensional response of the geomembranes has been investigated from a calculation of the volume changes of the samples due to swelling. The changes in thickness and diameter of the geomembrane samples have been calculated at different time intervals during soaking experiments. The thickness measurements (± 0.001 cm) were done using the micrometer screw gauge. Vernier callipers was used to measure the diameter within

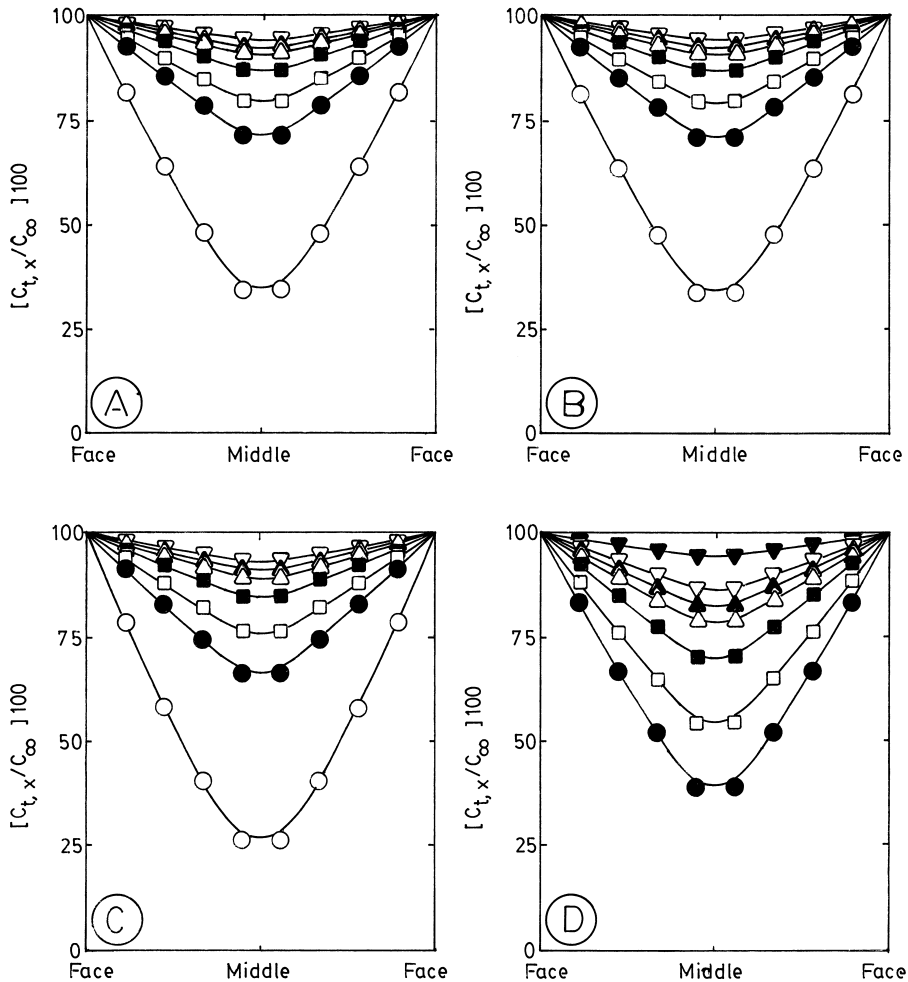

Fig. 10. Concentration profiles calculated from Eq. (7) for heptane with (A) PP, (B) VLDPE, (C) LLDPE and (D) HDPE geomembranes for the same time intervals as in Fig. 8 at 70°C.

an accuracy of ± 0.001 cm. The values of D based on volume changes are then calculated by using [13]:

$$C_t = \left(\frac{W_t}{W_0}\right) = \left(\frac{4W_\infty}{hW_0}\right)\left(\frac{D_v}{\pi}\right)^{1/2} t^{1/2} \tag{9}$$

where W_∞ is equilibrium weight of the samples and D_v is diffusion coefficient calculated from volume expansion of the samples. Assuming that increase in volume of the geomembrane at any given instant of time is proportional to the weight of the liquid sorbed up to that time so that we may write: $W_t \propto$ (swollen volume of the geomembrane

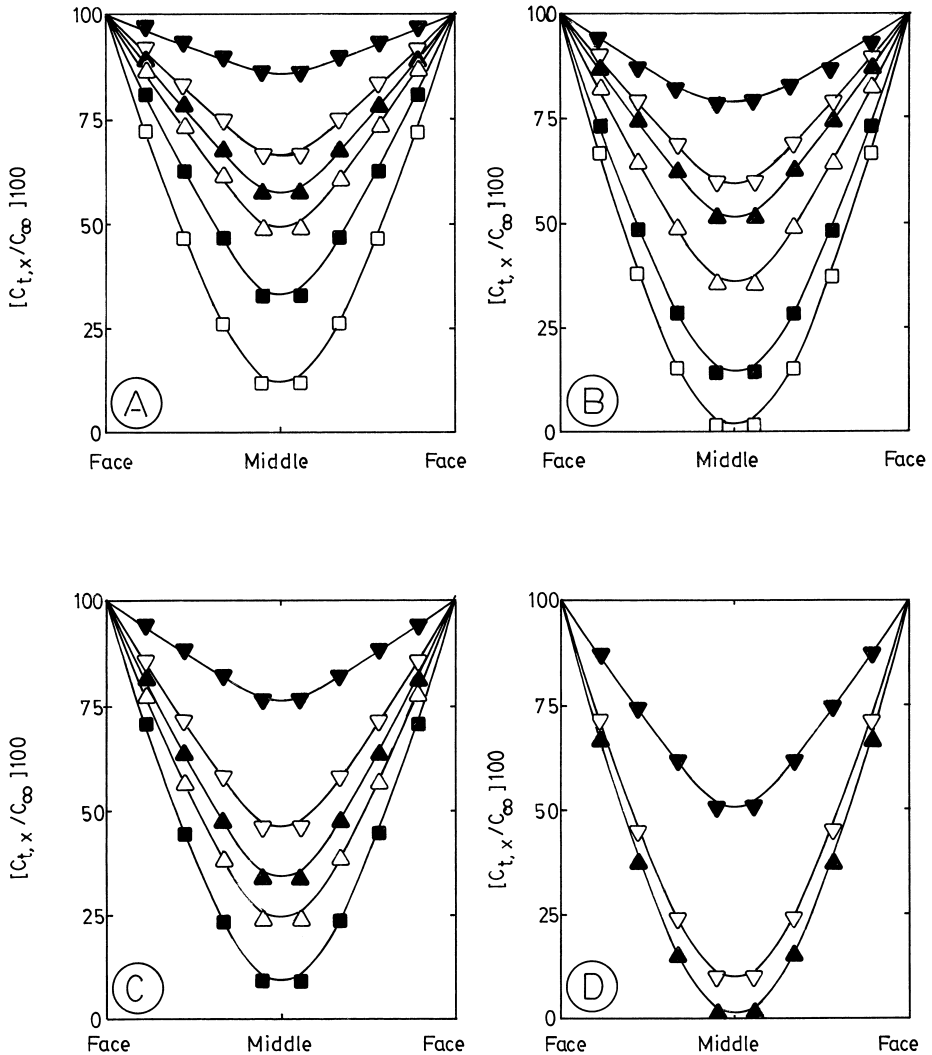

Fig. 11. Concentration profiles calculated from Eq. (7) for pentadecane with (A) PP, (B) VLDPE, (C) LLDPE and (D) HDPE geomembranes for the same time intervals as in Fig. 8 at 25°C.

at time t - initial volume of the geomembrane). Thus, the mass gain at time, t is calculated as:

$$W_t = b\pi\left(r_t^2 h_t - r_0^2 h_0\right) \tag{10}$$

$$W_\infty = b\pi\left(r_\infty^2 h_\infty - r_0^2 h_0\right) \tag{11}$$

where b is a proportionality constant and r_0, r_t and r_∞ are radii of the circular disc-shaped samples initially at zero time, after lapse of time, t and at equilibrium time

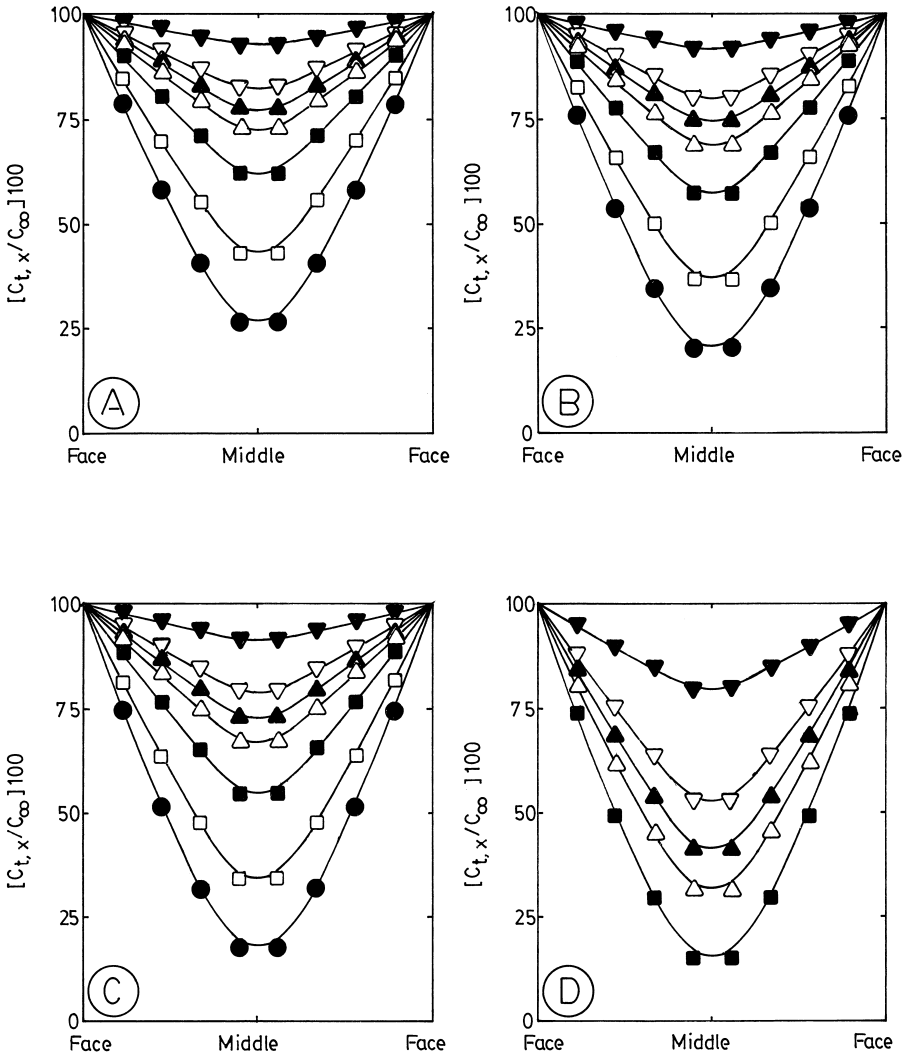

Fig. 12. Concentration profiles calculated from Eq. (7) for pentadecane with (A) PP, (B) VLDPE, (C) LLDPE and (D) HDPE geomembranes for the same time intervals as in Fig. 8 at 50°C.

respectively. Substituting the values of W_t and W_∞ into Eq. (9) we get,

$$\left(r_t^2 h_t - r_0^2 h_0\right) = \left(\frac{4\left(r_\infty^2 h_\infty - r_0^2 h_0\right)}{h}\right)\left(\frac{D_v}{\pi}\right)^{1/2} t^{1/2} \tag{12}$$

where $(r_t^2 h_t - r_0^2 h_0)$ and $(r_\infty^2 h_\infty - r_0^2 h_0)$ represent the volume changes at time, t (i.e. ΔV_t) and at equilibrium time (i.e. ΔV_∞). Thus, Eq. (12) can be rewritten as

$$\Delta V_t = \left(\frac{4\Delta V_\infty}{h}\right)\left(\frac{D_v}{\pi}\right)^{1/2} t^{1/2} \tag{13}$$

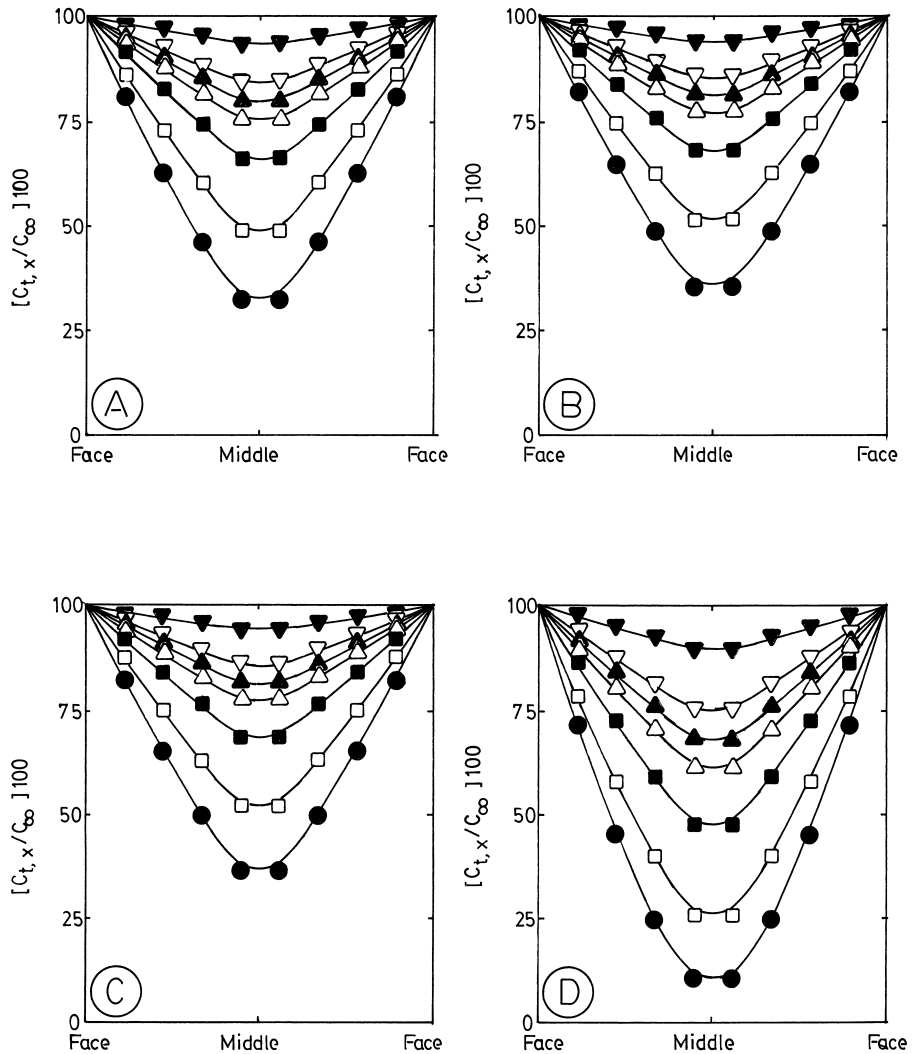

Fig. 13. Concentration profiles calculated from Eq. (7) for pentadecane with (A) PP, (B) VLDPE, (C) LLDPE and (D) HDPE geomembranes for the same time intervals as in Fig. 8 at 70°C.

For the changes in volume per unit volume, Eq. (13) becomes

$$\left(\frac{\Delta V_t}{V_0}\right) = \left(\frac{4\left(\frac{\Delta V_t}{V_0}\right)}{h}\right)\left(\frac{D_v}{\pi}\right)^{1/2} t^{1/2} \tag{14}$$

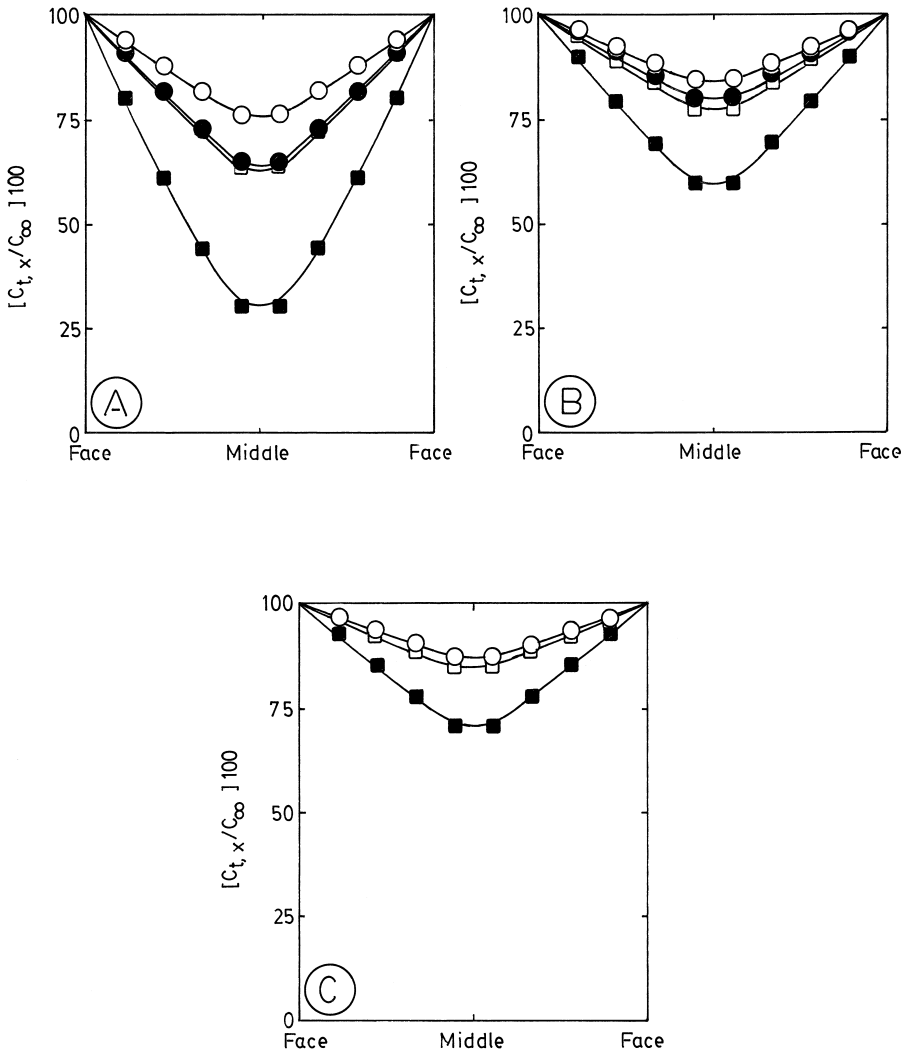

Fig. 14. Concentration profiles calculated from Eq. (7) for heptane with PP (○); VLDPE (●); LLDPE (□); and HDPE (■); at (A) 25°C, (B) 50°C and (C) 70°C for 20 min sorption.

The expression for diffusion coefficient, D_v may then be written as:

$$D_v = \pi \left(\frac{\theta h}{4 \Delta V_m} \right)^2 \tag{15}$$

where θ is slope of the $\Delta V_t / V_0$ vs. $t^{1/2}$ plots.

Swelling curves for PP geomembranes at 25°C are presented in Fig. 16. The dependence of percentage increase in thickness and diameter in addition to percentage volume swell data of the geomembrane samples are also presented. Due to insignificant

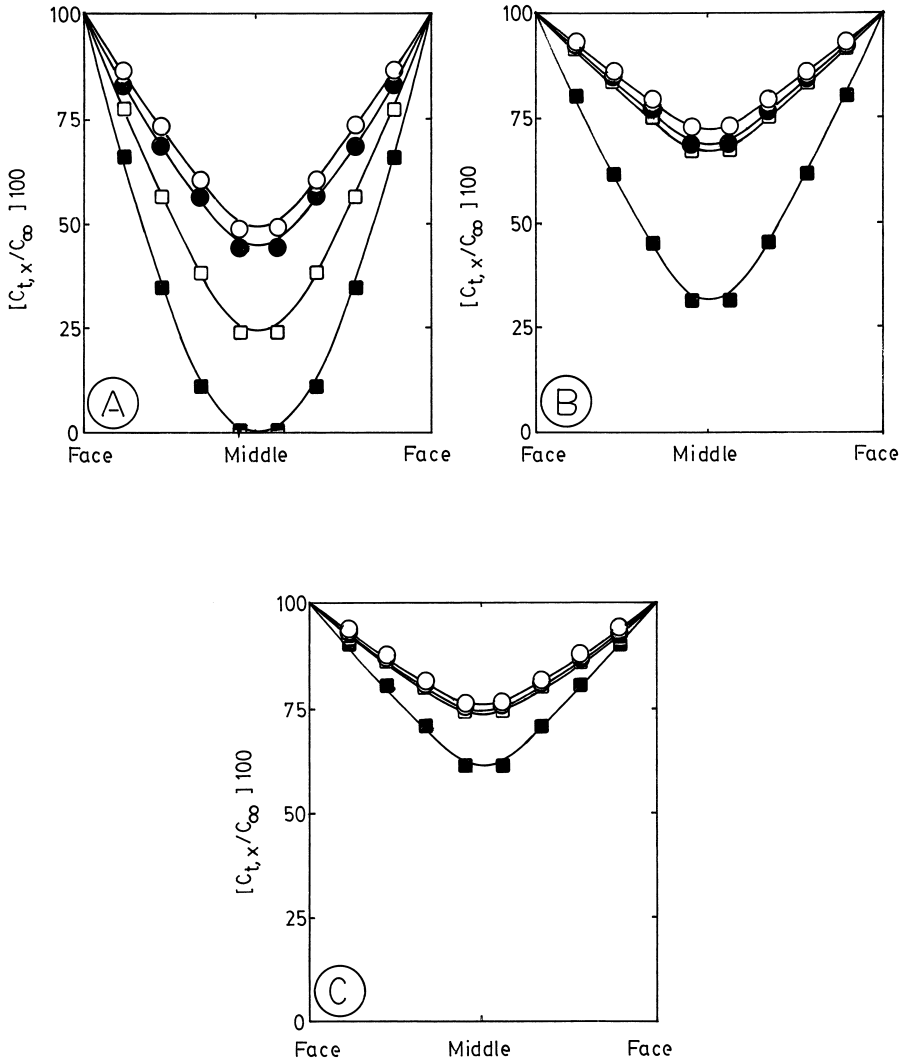

Fig. 15. Concentration profiles calculated from Eq. (7) for pentadecane with PP (○); VLDPE (●); LLDPE (□) and HDPE (■) at (A) 25°C, (B) 50°C and (C) 70°C for 40 min sorption.

swelling of the polyethylene-based geomembranes, such swelling curves are not presented for these geomembranes. Swelling results expressed as maximum percentage increase in thickness, Δh_∞ and diameter, Δd_∞ are presented in Table 5 only in the case of PP geomembrane. Since, no increase in thickness or diameter for the polyethylene-based geomembranes is observed, these data were not obtained. In general, equilibrium swelling is higher for heptane than hexane in the case of PP geomembrane. However, for the other alkanes equilibrium swelling decreases with increasing size of *n*-alkanes

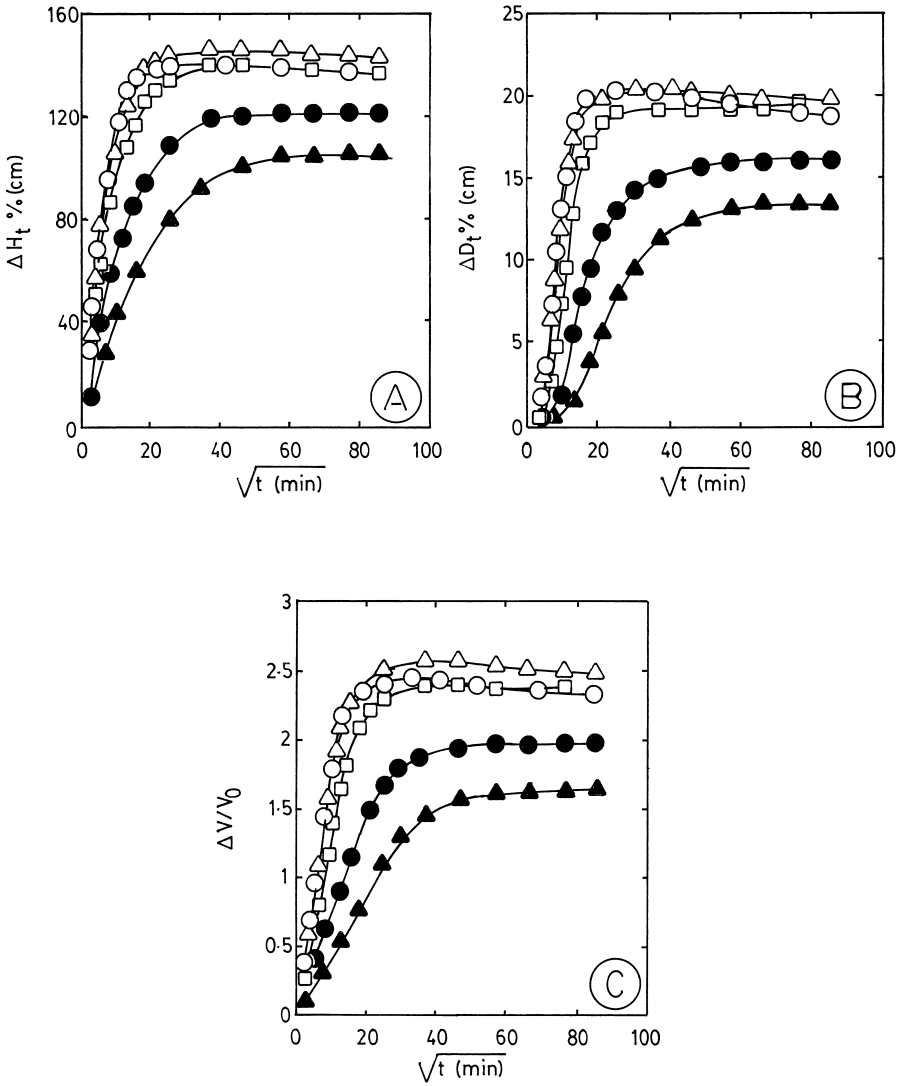

Fig. 16. Percentage increase in thickness (Δh), diameter (Δd) and increase in volume (ΔV_m) vs. square root of time ($t^{1/2}$) for PP geomembrane with (○) hexane, (△) heptane, (□) nonane, (●) dodecane and (▲) pentadecane at 25°C.

i.e. equilibrium swelling of pentadecane is lower than all the other alkanes showing a clear-cut dependence of swelling on the size of *n*-alkane molecules.

From a least-squares analysis of the slope of the linear portion (i.e. before 55% swelling equilibrium) of the volume swelling curves presented in Fig. 16, the values of D_v have been calculated using Eq. (15) and these are also included in Table 5 along with the swelling index data calculated as: $\alpha = (\Delta h_\infty d_0)/(\Delta d_\infty h_0)$. The values of α are

Table 5
Percent maximum increase in thickness, Δh_∞ (cm), diameter, Δd_∞ (cm) and volume (ΔV_∞), diffusivity for volume change, D_v (10^7 cm^2/s), swelling index, α (cm^3/g) at equilibrium

n-Alkanes	PP geomembrane				
	Δh_∞	Δd_∞	ΔV_∞	D_v	α
Hexane	141.30	20.68	2.48	1.69	7.29
Heptane	146.01	20.65	2.59	2.45	7.22
Nonane	140.10	19.50	2.40	1.04	7.08
Dodecane	121.36	15.96	1.98	0.55	7.57
Pentadecane	114.25	13.36	1.65	0.26	7.88

almost identical for all the *n*-alkanes and vary from 7.08 to 7.88. The values of D_v are smaller than those of D obtained from sorption experiments. This may be explained in terms of free volume considerations [26,27]. If the available free volume spaces between polymer segments are bigger than the solvent molecules, then the liquid entering into these spaces may not cause significant change in volume. On the other hand, when the *n*-alkanes do not enter into the already available free volume, then the polymer segments tend to relax and thereby contribute toward swelling. In the absence of any such interactions between the polymer segments and *n*-alkanes at any time *t*, the mass uptake by the geomembrane may not be equivalent to the corresponding volume gain. This further results in a decrease in the values of volume gain when compared to mass gain results. Therefore, the diffusion coefficients calculated from mass gain measurements are higher than those obtained from dimensional response measurements.

4.5. Arrhenius activation parameters

Diffusion data of the geomembrane–alkane systems increase with increasing temperature and hence, attempts have been made to calculate the energy of activation for diffusion Arrhenius plots of ln D vs. $1/T$. In all the cases, Arrhenius plots exhibit linearity (Fig. 17) and this suggests that the values of activation energy for diffusion, E_D are roughly constant over the investigated range of temperature. The E_D values have been estimated from least-squares method by fitting the ln D data vs. $1/T$ using the following Arrhenius relation:

$$\ln D = \ln D_0 - \frac{E_D}{RT} \tag{16}$$

In a similar manner, the results of S have been used to estimate the heat of sorption, ΔH_S using the relation:

$$\ln S = \ln S_0 - \frac{\Delta H_S}{RT} \tag{17}$$

In the above equation, D_0 and S_0 represent the constant terms, R is gas constant and T is absolute temperature. The estimated values of E_D and ΔH_S for all the systems are presented in Table 6. In the case of PP geomembrane, the E_D values increase from 25 to

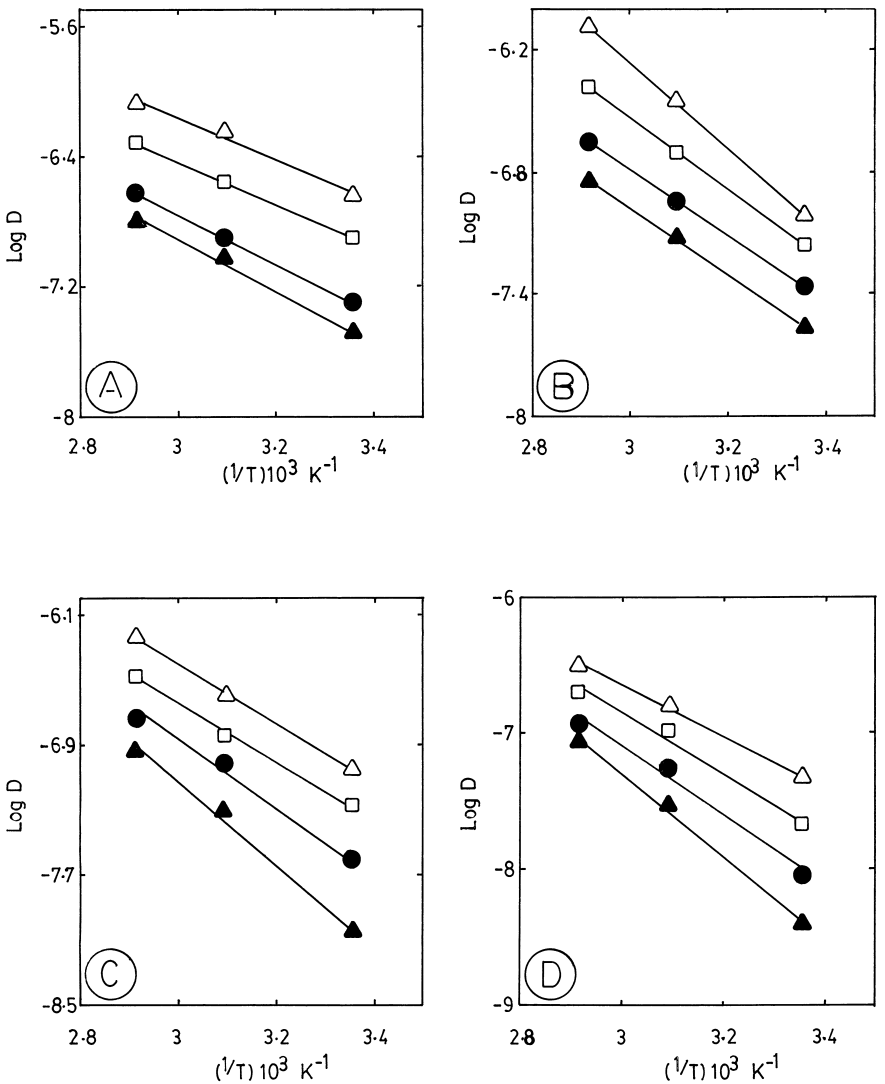

Fig. 17. Arrhenius plots of ln D vs. $1/T$ for (A) PP, (B) VLDPE, (C) LLDPE and (D) HDPE geomembranes with *n*-alkanes, symbols are the same as in Fig. 1.

31 kJ/mol, whereas for VLDPE there is a decrease in E_D values which range from 40 to 31 kJ/mol from heptane to pentadecane. In the case of LLDPE and HDPE geomembranes these values increase with the size of alkanes and the E_D values for HDPE are higher than all the other geomembranes. The results of ΔH_S for PP and HDPE geomembranes are smaller than LLDPE and VLDPE geomembranes and these values vary from 10 to 13 kJ/mol. This further suggests that the results of ΔH_S and E_D are dependent more on the nature of the geomembrane than the size of the penetrating

Table 6
Activation energy for diffusion (E_D in kJ/mol), heat of sorption (ΔH_S in kJ/mol) and heat of mixing (ΔH_{mix} in kJ/mol) for geomembranes with *n*-alkanes

n-Alkanes	ΔH_v[a]	Property	PP	VLDPE	LLDPE	HDPE
Heptane	37.36	E_D	24.8 ± 2.5	40.2 ± 0.8	35.6 ± 1.0	37.8 ± 3.5
		ΔH_S	10.3 ± 0.3	27.2 ± 3.1	18.7 ± 2.0	13.0 ± 0.8
		ΔH_{mix}	47.7 ± 0.3	64.6 ± 3.1	56.1 ± 2.0	50.4 ± 0.8
Nonane	43.75	E_D	25.0 ± 0.1	33.4 ± 0.6	34.4 ± 2.1	43.9 ± 9.0
		ΔH_S	10.8 ± 0.2	26.6 ± 5.7	19.9 ± 1.9	13.2 ± 0.6
		ΔH_{mix}	54.6 ± 0.2	70.4 ± 5.7	63.7 ± 1.9	57.0 ± 0.6
Dodecane	49.61	E_D	29.6 ± 0.2	31.1 ± 0.2	38.6 ± 4.8	50.9 ± 17
		ΔH_S	11.8 ± 0.1	20.0 ± 6.9	18.2 ± 2.8	12.5 ± 0.3
		ΔH_{mix}	61.4 ± 0.1	69.6 ± 6.9	67.8 ± 2.8	62.1 ± 0.3
Pentadecane	[b]	E_D	30.8 ± 3.1	31.7 ± 1.1	51.0 ± 6.6	60.5 ± 0.4
		ΔH_S	13.2 ± 2.7	10.1 ± 3.9	11.5 ± 5.1	10.6 ± 4.0
		ΔH_{mix}	[c]	[c]	[c]	[c]

[a] These values (in kJ/mol) were taken from the CRC Handbook of Chemistry and Physics (Weast), 67th edn., CRC Press, Boca Raton, FL, 1986–1987.
[b] Data not available.
[c] Data not calculated.

alkane molecules. The heat of sorption being positive in all the cases, suggests that the heat of condensation is positive and greater in magnitude than the heat of mixing ΔH_{mix} which can be calculated according to the relation [30]:

$$\Delta H_{mix} = \Delta H_S + \Delta H_v \tag{18}$$

where ΔH_v is heat of vaporization. These ΔH_{mix} values presented in Table 6 show an increasing trend from heptane to pentadecane suggesting a driving force increase with increasing length of *n*-alkanes.

5. Conclusions

In field applications, the barrier geomembranes with lower liquid sorption/diffusion properties are needed not only for liquid storage, but also to dispose off the hazardous wastes. Such barrier materials with better liquid resistivity properties have good applications as liners in hazardous waste pond applications to prevent the transport of leachates or liquids in the wastes, thereby alleviating the pollution of ground water. In the absence of actual field experience on long-term performance of geomembranes, preliminary laboratory data of the kind presented here are useful. However, it is possible that the geomembranes may be subjected to a variety of pollutants that may adversely affect their performance due to chemical degradation, swelling and environmental stress cracking. These aspects need to be well understood before their successful applications.

The goal of the present research is to identify factors that are responsible for predicting the long-term performance of HDPE, LLDPE, VLDPE and PP geomembranes with *n*-alkanes. Sorption and diffusion data are obtained at 25, 50 and 70°C, while

desorption and swelling results were obtained at 25°C. The temperature dependence of these parameters indicate that the activation energy of diffusion and heat of sorption are dependent on the type of the geomembrane used and the nature of liquid environment.

Ultimately, the choice of geomembrane depends upon the type of the hazardous chemical to be retained. Among many criteria used to assess the compatibility of geomembranes, one of the most useful parameters is its interaction with the liquid environments. In addition, weight, volume, mechanical properties and hardness changes of the geomembrane are also important. Generally, a geomembrane is considered acceptable for lining applications if it undergoes less than 10% weight or volume change and less than 10 point Durometer hardness change after 30 days of exposure in the selected environment. It was found that the chemical resistivity of a geomembrane depends on polymer structure, molecular weight, crystallinity and degree of cross-linking, if any. Chemical compatibility testing of these materials must be performed both to meet the designers need to support the material selection decision and to provide documentation for the facility operating permit application.

Acknowledgements

We thank the Department of Science and Technology, New Delhi (SP/S1/H-26/96(PRU)) for a major financial support to buy the equipments used in this study. Gratitude is extended to Mr. Jack Donaldson and Mr. John Siebken of National Seal, 1255 Manmouth Blvd., Galesburg, IL, USA for a supply of geomembranes.

References

[1] M. Cadwallader, Chemical compatibility considerations for HDPE liners in waste containment, Paper presented at the Am. Inst. Chem. Eng. National Meeting, Boston, MA, USA, 24–27 August, 1986.
[2] P.E. Cassidy, M. Mores, D.J. Kerwick, D.J. Koeck, K.L. Verschoor, D.F. White, Chemical resistance of synthetic materials, Geotextiles Geomembranes 11 (1992) 61–98.
[3] J. Cooke, L. Rebenfeld, Geotextiles Geomembranes 7 (1988) 7–22.
[4] H.E. Haxo, Jr., J.A. Miedema, N.A. Nelson, Permeability of polymeric membrane lining materials, Proceedings of the International Conference on Geomembranes, Vol. 1, Denver, CO, USA, June 20–24, 1984, pp. 151–168.
[5] H.E. Haxo Jr., J.A. Miedema, N.A. Nelson, Permeability of polymeric membrane lining materials for waste management facilities, Elastomerics 117 (1985) 29–37.
[6] H.E. Haxo, Jr., Determining the transport through geomembranes of various permeants in different applications, Geosynthetic Testing For Waste Containment Applications, Las Vegas, NV, USA, ASTM Special Technical Publication 1081, Philadelphia, PA, USA, 1990, pp. 75–94.
[7] N.M.W. John, Geotextiles, Blakie & Sons, London, 1987.
[8] R. Koerner, Designing with Geosynthetics, Prentice-Hall, Englewood Cliffs, NJ, USA, 1990.
[9] J.D. Ortego, T.M. Aminabhavi, S.F. Harlapur, R.H. Balundgi, A review of polymeric geosynthetics used in hazardous waste facilities, J. Hazard. Mater. 42 (1995) 115–156.
[10] J. Stastna, D. De Kee, Transport Properties in Polymers, Technomic Publishing, Lancaster, USA, 1995.
[11] J. Crank, The Mathematics of Diffusion, 2nd edn., Clarendon Press, Oxford, 1975.
[12] U.S. Aithal, T.M. Aminabhavi, Measurement of diffusivity of organic liquids through polymeric membranes—A simple inexpensive laboratory experiment, J. Chem. Educ. 67 (1990) 82–85.

[13] T.M. Aminabhavi, U.S. Aithal, S.S. Shukla, An overview of theoretical models used to predict transport of small molecules through polymer membranes, J. Macromol. Sci. Revs. Macromol. Chem. Phys. C 28 (3 and 4) (1988) 421–474.
[14] T.M. Aminabhavi, S.F. Harlapur, R.H. Balundgi, J.D. Ortego, Sorption kinetics and diffusion of alkanes into tetrafluoroethylene/propylene copolymer membranes, J. Appl. Polym. Sci. 59 (1996) 1857–1870.
[15] T.M. Aminabhavi, S.B. Harogoppad, Kinetic and thermodynamic study on the sorption of liquids by polymer films. A simple laboratory experiment, J. Chem. Educ. 68 (1991) 343–346.
[16] T.M. Aminabhavi, R.S. Munnolli, Sorption and diffusion of aldehydes and ketones into elastomers, Polym. Int. 32 (1993) 61–70.
[17] T.M. Aminabhavi, R.S. Munnolli, Molecular transport of organic esters and ketones into fluoropolymer membranes, Can. J. Chem. Eng. 72 (1994) 1047–1054.
[18] T.M. Aminabhavi, R.S. Munnolli, Molecular transport characteristics of chlorosulfonated polyethylene geomembrane in the presence of aromatic esters, J. Chem. Technol. Biotechnol. 63 (1995) 69–77.
[19] T.M. Aminabhavi, R.S. Munnolli, J.D. Ortego, Sorption and diffusion of *n*-alkanes into bromobutyl rubber membranes, Polym. Int. 36 (1995) 353–363.
[20] T.M. Aminabhavi, R.S. Munnolli, J.D. Ortego, Interactions of chlorosulfonated polyethylene geomembranes with aliphatic esters: Sorption and diffusion phenomena, Waste Manage. 15 (1995) 69–78.
[21] T.M. Aminabhavi, H.T.S. Phayde, Molecular transport of alkanes through thermoplastic miscible blends of ethylene–propylene random copolymer and isotactic polypropylene, J. Appl. Polym. Sci. 55 (1995) 1335–1352.
[22] T.M. Aminabhavi, H.T.S. Phayde, Molecular transport characteristics of Santoprene thermoplastic rubber in the presence of aliphatic alkanes over the temperature interval of 25 to 70°C, Polymer 6 (1995) 1023–1033.
[23] T.M. Aminabhavi, H.T.S. Phayde, J.D. Ortego, J.M. Vergnaud, A study of sorption/desorption profiles and diffusion anomalies of organic haloalkanes into a polymeric blend of ethylene–propylene random copolymer and isotactic polypropylene, Polymer 37 (1996) 1677–1684.
[24] S.B. Harogoppad, T.M. Aminabhavi, Diffusion and sorption of organic liquids through polymer membranes: 5. Neoprene, styrene–butadiene–rubber, ethylene–propylene–diene–terpolymer and natural rubber versus hydrocarbons, Macromolecules 24 (1991) 2598–2605.
[25] J.M. Vergnaud, Liquid Transport Processes in Polymeric Materials, Modeling and Industrial Applications, Prentice-Hall, Englewood Cliffs, NJ, 1991.
[26] J.S. Vrentas, J.L. Duda, Solvent and temperature effects on diffusion in polymer–solvent systems, J. Appl. Polym. Sci. 21 (1977) 1715–1728.
[27] H. Fujita, A. Kishimoto, K.M. Matsumoto, JCS, Trans. Faraday Soc. 56 (1960) 424–437.
[28] N.M. Franson, N.A. Peppas, Influence of copolymer composition on non-Fickian water transport through glassy copolymers, J. Appl. Polym. Sci. 28 (1983) 1299–1310.
[29] L.M. Lucht, N.A. Peppas, Transport of penetrants in the macromolecular structure of coals, J. Appl. Polym. Sci. 33 (1987) 1557–1566.
[30] J.H. Hildebrand, R.L. Scott, The Solubility of Nonelectrolytes, 3rd edn., Reinhold, New York, 1950.